Polarization control of spontaneous emission for rapid quantum-state initialization

C. S. DiLoreto[1] and C. Rangan[1,2]
[1]*Department of Physics, University of Windsor, Windsor ON, Canada N9B3P4*
[2]*Department of Physics, The University of Michigan, Ann Arbor, Michigan 48109, USA*
(Received 5 August 2016; published 21 April 2017)

We propose an efficient method to selectively enhance the spontaneous emission rate of a quantum system by changing the polarization of an incident control field, and exploiting the polarization dependence of the system's spontaneous emission rate. This differs from the usual Purcell enhancement of spontaneous emission rates as it can be selectively turned on and off. Using a three-level Λ system in a quantum dot placed in between two silver nanoparticles and a linearly polarized, monochromatic driving field, we present a protocol for rapid quantum state initialization, while maintaining long coherence times for control operations. This process increases the overall amount of time that a quantum system can be effectively utilized for quantum operations, and presents a key advance in quantum computing.

DOI: 10.1103/PhysRevA.95.043834

I. INTRODUCTION

The practical implementation of quantum computers [1] places two specific requirements on the lifetime of a qubit, namely, long relevant decoherence times, and rapid state initialization times. A great deal of recent research has been devoted to proposing solutions that minimize the overall spontaneous emission rate and preserve system purity [2–6]. These decoherence-minimization processes lead to longer effective qubit operational lifetimes, but decoherence will ultimately render the qubit unusable due to loss of state purity. The simplest way to restore system purity is to wait for the system to cool to a pure state, usually the ground state. Therefore for practical, reusable qubits, it is useful to design systems in which the time to cool to the ground state is minimized [7]. This time is typically quite large since the quantum state's lifetime is selected to be very large with respect to the time scales of the control processes, i.e., the spontaneous emission rate is selected to be quite low. Thus, the desires for long operational times and short cooling times of a qubit place contradictory demands on the spontaneous emission rate of the quantum excited state. There is a need for protocols wherein the spontaneous emission rate of a quantum system can be selectively decreased so that long state lifetimes can be maintained during operation, and upon demand, selectively increased so that the cooling time can be drastically shortened in duration when qubit purity needs to be restored. Recent experiments have increased the spontaneous emission rate of a quantum excited state by coupling the system to a nearby resonant structure such as a cavity [8–13], photonic crystal [14], or nanoparticle [15] based on the Purcell effect [16]. However, these studies have not been able to toggle a system between a configuration where the spontaneous emission rate is low (for qubit operation) and high (for qubit initialization).

In this paper, we propose a scheme to enhance the spontaneous emission rate of a quantum state "on demand," so that quantum states can be rapidly initialized (so-called "rapid reset") without shortening their operational lifetimes. In our scheme, a quantum system (such as a quantum dot) is placed in between a pair of noble-metal nanoparticles, and controlled by a linearly polarized electromagnetic wave that propagates perpendicularly to the interparticle axis. The local surface-plasmon resonance phenomenon and the accompanying enhancement of the local field around noble-metal nanostructures is well known [17–19]. It is also well known that the spontaneous emission rate of a quantum emitter in the middle of two Ag nanoparticles is enhanced and is strongly frequency dependent, thus applied to surface-enhanced fluorescence [20–22]. It is less well known that the modification of the spontaneous emission rate due to the weak coupling to the surface-plasmon modes exhibits a strong dependence on the polarization of the incident light [23–25]. In the scheme we describe below, changing the polarization direction of the electromagnetic wave from perpendicular to the interparticle axis to parallel to the interparticle axis changes the spontaneous emission rate of a quantum emitter at a particular wavelength from very low to very high. We use this effect to develop a protocol wherein one of the arms of a three-level Λ system (3LLS) can be used as a qubit that has a long coherence lifetime during the operational mode, and quickly reset to a pure state when the qubit becomes unusable due to decoherence.

II. THEORETICAL METHODS

In our calculations, a radiating dipole (modeling a quantum dipole transition in a qubit) is placed equidistantly between two spherical Ag nanoparticles, of radius r and surface-to-surface separation d as shown in the inset in Fig. 1(a). The resonance spectra of these nanoparticles (NPs) can be tuned by changing their size and composition [26], allowing for a wide variety of quantum systems to be used as a qubit platform. We assume that the dipole is oriented by the polarization of an electromagnetic wave that illuminates the nanoparticles. We examine two cases—firstly when the dipole is oriented perpendicular to the interparticle axis ($\hat{z}$), and secondly when the dipole is oriented parallel to the interparticle axis ($\hat{x}$).

Figure 1 shows the modification of (a) the local electromagnetic field and (b) of the spontaneous emission rate of a quantum emitter placed in between two silver nanoparticles when the electromagnetic wave illuminating the system is $\hat{x}$ polarized parallel to the interparticle axis (red, dashed line), and $\hat{z}$ polarized perpendicular to the interparticle axis (blue,

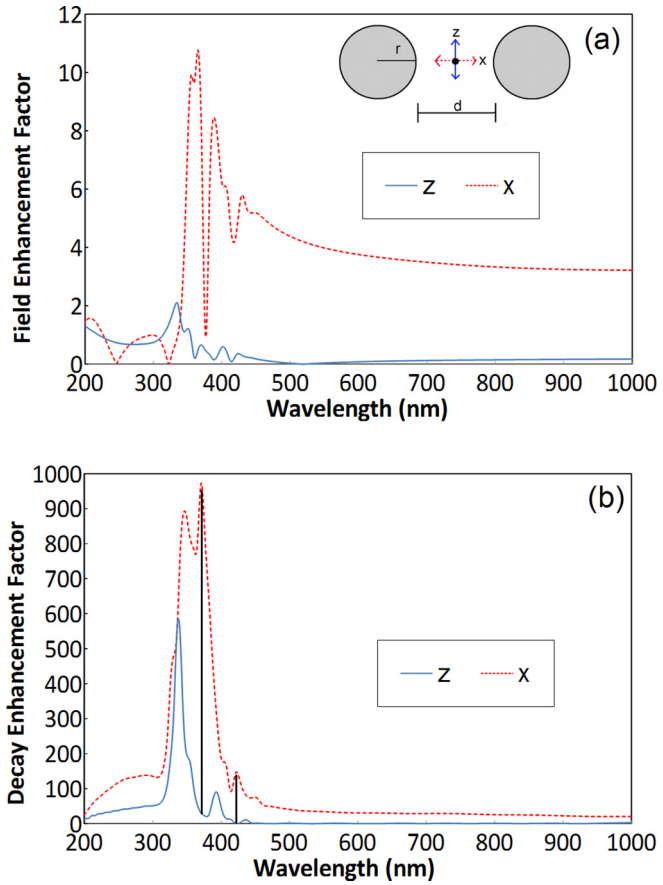

FIG. 1. (a) Field enhancements ($M_{E,i} = |E_i|/E_0$) and (b) decay rate modification ($M_d = \gamma/\gamma_0$) of the quantum emitter placed halfway in between two silver NPs with $r = 20$ nm and $d = 12$ nm surface-to-surface separation for two different incident polarizations. The blue, solid (red, dashed) curves correspond to when the incident field is perpendicular (parallel) to the interparticle axis. The two solid vertical lines in (b) correspond to the maximum decay rate enhancement for the $\hat{x}$ orientation (370 nm) and the largest relative ratio of decay rate enhancement, $\hat{x}/\hat{z}$ (≈420 nm).

solid line). The radius of the nanoparticles is chosen to be 20 nm and the interparticle surface-to-surface spacing as 12 nm so that the localized surface-plasmon resonance frequency, calculated to be 370 nm, matches the transition frequency of the qubit. This frequency is similar to transition frequencies found in ultraviolet quantum dots such as ZnO [27] and due to the tunability of both the nanoparticle resonance and the qubit energy-level spacing such a frequency choice serves as a good model to illustrate how polarization control can speed up qubit initialization.

The local electromagnetic field vector components (E_x, E_y, E_z) at the location of the quantum emitter (halfway in between the nanoparticles on the interparticle axis) due to the driving fields are calculated numerically by solving Maxwell's equations for different incident-field polarizations. A commercial-grade simulator based on the finite-difference time domain method was used to preform the calculations [28]. The optical response of the material is determined via the Drude model using experimental constants [29]. The magnitude of the incident electric field is assumed to be E_0 in both polarizations. We define a "field-enhancement factor" $M_{E,i} = |E_i|/E_0$, distinct from the intensity magnification factors usually reported in studies of surface-enhanced processes. Figure 1(a) shows the field-enhancement factors in the $\hat{z}$ (blue, solid line) and $\hat{x}$ (red, dashed line) components of the field when the incident light is polarized in the same ($\hat{z}$ or $\hat{x}$) direction. These two curves show that the presence of the nanoparticles greatly enhances the field strength in the direction of polarization of the incident light. Thus, the driven qubit is driven much harder (or the Rabi frequency increases) due to the presence of the proximate nanoparticles.

The rate of spontaneous emission of the quantum emitter changes when placed in between the two silver nanoparticles (AgNPs). This change in the rate of spontaneous emission is calculated by modeling the quantum emitter as a point oscillating dipole source. We compare the power emitted by the point dipole source with (P_{NP}), and without the nanoparticles ($P_{\mathrm{No\,NP}}$) [15] by solving Maxwell's equations numerically [28]. The decay-enhancement factor M_d is calculated as a ratio of P_{NP} to $P_{\mathrm{No\,NP}}$ immediately around the dipole source. This decay-enhancement factor is also the ratio of the spontaneous emission rate of the dipole emitter with the nanoparticles γ to the vacuum spontaneous emission rate γ_0 [23]. The decay-enhancement factor as a function of wavelength is evaluated for two different orientations of the dipole; one in which the dipole is perpendicular to the interparticle axis ($\hat{z}$) and the other in which it is parallel to the interparticle axis ($\hat{x}$), and presented in Fig. 1(b). We see that at wavelengths near the qubit resonance, the rate of spontaneous emission of the quantum emitter can be increased by switching from z to x polarization.

Thus the polarization of the driving field both modifies the Rabi frequency and the spontaneous decay rate of the qubit transition parallel to it. Based on the above analysis, the wavelength of the incident electromagnetic wave is chosen so that the ratio of parallel decay rate (γ_x) to the perpendicular decay rate (γ_z) is maximized (≈420 nm).

III. IMPLEMENTATION PROTOCOL

For a practical qubit implementation, we offer the following protocol:

Step 1. Consider a three-level quantum system in the Λ configuration (3LLS), with both ground states $|g\rangle$ and $|c\rangle$ being somewhat close in energy though not degenerate. The lifetime of the excited state $|e\rangle$ is long enough for the quantum system to be a good candidate for quantum information processing. This system can then be placed in between two silver nanoparticles. The two ground states, $|g\rangle$ and $|c\rangle$, are chosen as the qubit, and gate operations are carried out by a near-resonant electromagnetic wave polarized in the $\hat{z}$ direction—perpendicular to the interparticle axis. This allows the rate of spontaneous emission from the excited states, $\gamma_{ge,z}$ and $\gamma_{ce,z}$, to remain fairly low. Without loss of generality, one can assume that the ground states are angular momentum $j = 0$ states, and the excited state is a $j = 1$ state, thus the applied linearly polarized field transitively connects the $|g, j = 0, m = 0\rangle$ state with the $|e, j = 1, m = 0\rangle$ state.

Step 2. When the qubit becomes unusable due to decoherence, and the state needs to be initialized, the polarization of

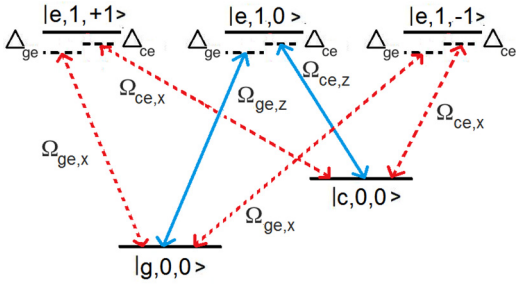

FIG. 2. Polarization control scheme for rapid qubit initialization. Two applied fields near resonant with the $|g\rangle$-$|e\rangle$ and $|c\rangle$-$|e\rangle$ transitions are linearly polarized in the x-z plane. The z components of the field excite the blue (solid) transitions, while the x components of the field excite the red (dashed) transitions. For preparation, the Rabi frequencies of all transitions are high with respect to spontaneous decay rates. The spontaneous emission rates of the operational (blue, solid) transitions, $\gamma_{ge,z}$ and $\gamma_{ce,z}$, stay low, whereas those of the preparation transitions (red, dashed), $\gamma_{ge,x}$ and $\gamma_{ce,x}$, are greatly enhanced. The detunings are chosen to coherently trap the system in a dark state.

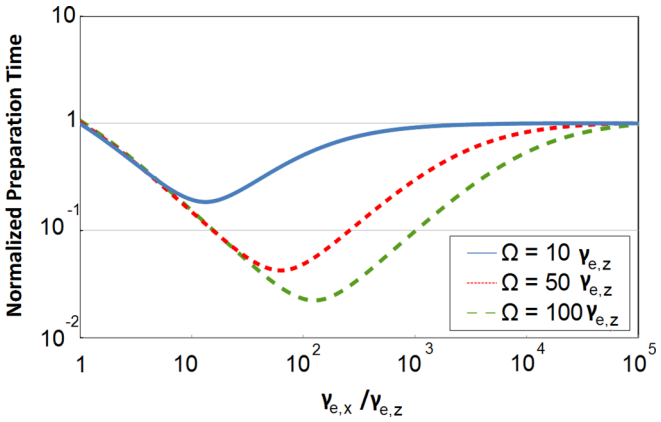

FIG. 3. The time required to reach a final, pure state is plotted with respect to the ratio of spontaneous decay rates ($\gamma_{ge,x}/\gamma_{ge,z} = \gamma_{ce,x}/\gamma_{ce,z}$) for various driving field strengths. The effective five-level system is initially driven from an operational, completely mixed state ($\rho_{gg} = \rho_{(e,0)(e,0)} = \rho_{cc} = \frac{1}{3}$). The calculation parameters are $\Omega_{ce,x} = \Omega_{ge,x} = \Omega_{ce,z} = \Omega_{ge,z}$, $\gamma_{ge,x} = \gamma_{ce,x} = \gamma_{e,x}$, and $\gamma_{ge,z} = \gamma_{ce,z} = \gamma_{e,z}$. The preparation time is normalized to the time taken for an equivalent three-level λ system to reach a steady state.

the incident electromagnetic wave is rotated by 45° to excite both along the $\hat{z}$ and $\hat{x}$ directions. Polarization selection rules create a five-level system transitively connected as shown in Fig. 2. The z-polarized components continue to connect the $|g, j = 0, m = 0\rangle$ and $|c, j = 0, m = 0\rangle$ states with the $|e, j = 1, m = 0\rangle$ state, and the spontaneous emission stays low (blue, solid lines). The x-polarized components connect the $|g, j = 0, m = 0\rangle$ state and $|c, j = 0, m = 0\rangle$ with the $|e, j = 1, m = \pm 1\rangle$ states, and the spontaneous emission from the latter states are high (red, dashed lines).

If the detunings of both transitions are kept equal $\Delta_{ge} = \Delta_{ce}$, a Morris-Shore [30,31] transformation shows that these transition dipole couplings put the 3LLS into a dark state [32,33], i.e., a superposition of the two ground states of the five-level system, which is a pure state. Thus, regardless of the initial quantum state of the system, the state can be rapidly reset into a pure state, i.e., the dark state.

Step 3. The rest of the qubit initialization can be completed by rotating the polarizations of the two electromagnetic waves perpendicular to the interparticle axis. In this configuration, the spontaneous emission from the excited state $|e\rangle$ is low, and population can be transferred coherently to the qubit ground state $|g\rangle$.

Rate of state initialization

The speed of state initialization is determined by the time that it takes the system to reach a steady state (the dark state) in Step 2. Although there are six different decay rates (one for each transition in Fig. 2), the overall time taken to reach the dark state depends mostly on the *fastest* spontaneous decay constant, especially if that decay time is much faster than the others. This means that if, due to the presence of a plasmonic nanostructure, only one decay rate is enhanced greatly, the entire preparation time will be reduced. In order to demonstrate this numerically, we use the Hamiltonian (assuming that the upper levels are degenerate) in the rotating-wave approximation:

$$H_{\mathrm{RWA}} = \begin{pmatrix} -\hbar\Delta_{ge} & \frac{\hbar\Omega_{ge,z}}{2} & \frac{\hbar\Omega_{ge,x}}{2} & \frac{\hbar\Omega_{ge,x}}{2} & 0 \\ \frac{\hbar\Omega^*_{ge,z}}{2} & 0 & 0 & 0 & \frac{\hbar\Omega_{ce,z}}{2} \\ \frac{\hbar\Omega^*_{ge,x}}{2} & 0 & 0 & 0 & \frac{\hbar\Omega_{ce,x}}{2} \\ \frac{\hbar\Omega^*_{ge,x}}{2} & 0 & 0 & 0 & \frac{\hbar\Omega_{ce,x}}{2} \\ 0 & \frac{\hbar\Omega^*_{ce,z}}{2} & \frac{\hbar\Omega^*_{ce,x}}{2} & \frac{\hbar\Omega^*_{ce,x}}{2} & -\hbar\Delta_{ce} \end{pmatrix}. \tag{1}$$

If the detunings of the applied fields from the two transitions are equal to each other ($\Delta_{ge} = \Delta_{ce}$), the population will be coherently trapped in the dark state. We assume that the ratios of the Rabi frequencies of the driven transitions are equal to each other, i.e., $\frac{\Omega_{e,x}}{\Omega_{e,z}} = \frac{\Omega_{c,x}}{\Omega_{c,z}}$. The rapidity with which the system reaches a ground state is determined by the relative magnitudes of the Rabi frequencies versus the decay rates of the transitions. If the Rabi frequencies are much greater than the decay rates, the system will rapidly reach the dark state.

As an example, we look at a 3LLS that, under the influence of decoherence in step 1, has evolved into a completely mixed state ($\rho_{gg} = \rho_{(e,0)(e,0)} = \rho_{cc} = \frac{1}{3}$).The time needed to reach the dark state (with calculated Purity $= \mathrm{Tr}(\rho^2) > 0.999\,999$) as a function of increasing spontaneous emission rate can be seen in Fig. 3 for varying driving field strengths. As the spontaneous emission rate of a transition increases, the time to reach the dark state decreases linearly. This happens until the time that the spontaneous emission rate is comparable to the Rabi frequency, and further increase in the spontaneous emission rate *increases* the time to reach the dark state. We see that the time needed for the system to reach the pure dark state decreases linearly with respect to the higher decay rate enhancement, even if that enhancement affects only a single transition and the system is initially in a state that is unaffected by that increased decay rate. However, once

the highest decay rate becomes greater than the driving Rabi frequency, this time reduction is lost as the fields are unable to drive significant population into these high decay states faster. This also indicates that this state initialization effect will only show up when the red (dashed) transitions are strongly driven. This allows for the preservation of low decoherence rates when the fields are only z polarized.

For the practical implementation of this protocol, some additional considerations may need to be accounted for. Firstly, in our calculations, we have assumed that the quantum emitter is a point dipole with no preferred quantization axis. This is not true in general for systems such as quantum dots, however, the protocol will succeed as long as the spontaneous emission rate of the system is asymmetric, i.e., significantly different for two orthogonal polarizations of the incident field. Secondly, we assume that the incident field is a plane wave, whereas in experiments, the field is likely to be a strongly focused beam for qubit addressing. The latter introduces an additional polarization (in the y direction), however, as the effects of the y-polarized components are similar to those of the z-polarized components due to the symmetry of the system, this will not substantially alter the ability to selectively enhance the preparation rate.

IV. CONCLUSION

In summary, we have proposed an elegant scheme to modify in real time the spontaneous emission rate of a quantum system through its interactions with local plasmonic nanostructures controlled by the polarization of an applied electromagnetic wave. Surface enhancements around plasmonic nanoparticles affect dipole transitions differently depending on the dipole's orientation. This difference can be used to selectively tune the spontaneous emission of a quantum dipole emitter. In a three-level Λ system (such as in a quantum dot) placed in between two Ag nanoparticles, varying the polarization of an incident driving electromagnetic wave can be used to go between a low spontaneous emission rate and a high spontaneous emission rate of the excited state. Thus, changing the polarization direction of the incident field allows one to use the quantum dot states in both operational mode (with low spontaneous emission) as well as to rapidly initialize or reset the system in a pure state, regardless of its initial conditions. This protocol for effective, rapid pure state preparation and state initialization represents a key improvement in the practical control of quantum information systems that are designed for continuous use and reuse.

ACKNOWLEDGMENTS

The authors gratefully acknowledge support from the Discovery Grant program of the Natural Sciences and Engineering Research Council of Canada (Grant No. 311880). Calculations were performed on the SharcNet supercomputing platform. We thank an anonymous referee for insightful comments on the practical implementation of this protocol.

[1] D. P. DiVincenzo, Fortschr. Phys. **48**, 771 (2000).
[2] E. J. Griffith, C. D. Hill, J. F. Ralph, H. M. Wiseman, and K. Jacobs, Phys. Rev. B **75**, 014511 (2007).
[3] M. Kleinmann, H. Kampermann, T. Meyer, and D. Bruß, Phys. Rev. A **73**, 062309 (2006).
[4] J. Bouda and V. Bužek, Phys. Rev. A **65**, 034304 (2002).
[5] J.-W. Pan, S. Gasparoni, R. Ursin, G. Weihs, and A. Zeilinger, Nature (London) **423**, 417 (2003).
[6] H. M. Wiseman and J. Ralph, New J. Phys. **8**, 90 (2006).
[7] M. A. Nielsen and I. L. Chuang, *Quantum Computation and Quantum Information* (Cambridge University Press, Cambridge, UK, 2000).
[8] P. Goy, J. M. Raimond, M. Gross, and S. Haroche, Phys. Rev. Lett. **50**, 1903 (1983).
[9] D. J. Heinzen, J. J. Childs, J. E. Thomas, and M. S. Feld, Phys. Rev. Lett. **58**, 1320 (1987).
[10] Y. Yamamoto, S. Machida, Y. Horikoshi, K. Igeta, and G. Bjrk, Opt. Commun. **80**, 337 (1991).
[11] A. Bienfait, J. J. Pla, Y. Kubo, X. Zhou, M. Stern, C. C. Lo, C. D. Weis, T. Schenkel, D. Vion, D. Esteve, J. J. L. Morton, and P. Bertet, Nature (London) **531**, 74 (2016).
[12] C. Jin, G. Wang, H. Wei, A.-T. Le, and C. Lin, Nat. Commun. **5**, 4003 (2014).
[13] T. B. Hoang, G. M. Akselrod, C. Argyropoulos, J. Huang, D. R. Smith, and M. H. Mikkelsen, Nat. Commun. **6**, 7788 (2015).
[14] N. Ganesh, W. Zhang, P. C. Mathias, E. Chow, J. Soares, V. Malyarchuk, A. D. Smith, and B. T. Cunningham, Nat. Nanotechnol. **2**, 515 (2007).
[15] H. Xu, X.-H. Wang, M. P. Persson, H. Q. Xu, M. Käll, and P. Johansson, Phys. Rev. Lett. **93**, 243002 (2004).
[16] E. M. Purcell, H. C. Torrey, and R. V. Pound, Phys. Rev. **69**, 37 (1946).
[17] E. J. Zeman and G. C. Schatz, J. Phys. Chem. **91**, 634 (1987).
[18] P. Rooney, A. Rezaee, S. Xu, T. Manifar, A. Hassanzadeh, G. Podoprygorina, V. Böhmer, C. Rangan, and S. Mittler, Phys. Rev. B **77**, 235446 (2008).
[19] S. M. H. Rafsanjani, T. Cheng, S. Mittler, and C. Rangan, J. Appl. Phys. **107**, 094303 (2010).
[20] E. Fort and S. Grésillon, J. Phys. D **41**, 013001 (2007).
[21] M. A. Antón, F. Carreño, S. Melle, O. G. Calderón, E. Cabrera-Granado, J. Cox, and M. R. Singh, Phys. Rev. B **86**, 155305 (2012).
[22] H. Xu, J. Aizpurua, M. Käll, and P. Apell, Phys. Rev. E **62**, 4318 (2000).
[23] L. Novotny and B. Hecht, *Principles of Nano-Optics* (Cambridge University Press, Cambridge, UK, 2006), pp. 281–282.
[24] K. Drexhage, J. Lumin. **1-2**, 693 (1970).
[25] H. Khosravi and R. Loudon, Proc. R. Soc. A **436**, 373 (1992).
[26] P. K. Jain, X. Huang, I. H. El-Sayed, and M. A. El-Sayed, Acc. Chem. Res. **41**, 1578 (2008).
[27] D. I. Son, B. W. Kwon, D. H. Park, W.-S. Seo, Y. Yi, B. Angadi, C.-L. Lee, and W. K. Choi, Nat. Nanotechnol. **7**, 465 (2012).
[28] Lumerical Solutions Inc., http://www.lumerical.com/tcad-products/fdtd.

[29] P. B. Johnson and R. W. Christy, Phys. Rev. B **6**, 4370 (1972).
[30] J. R. Morris and B. W. Shore, Phys. Rev. A **27**, 906 (1983).
[31] A. A. Rangelov, N. V. Vitanov, and B. W. Shore, Phys. Rev. A **74**, 053402 (2006).
[32] E. Arimondo, Coherent population trapping in laser spectroscopy, in *Progress in Optics*, Vol. 35, edited by E. Wolf (Elsevier, Amsterdam, 1996), pp. 257–354.
[33] H. R. Gray, R. M. Whitley, and C. R. Stroud, Opt. Lett. **3**, 218 (1978).